BATCH: la11a18 USER: sst29 DIV: @xyv04/data1/CLS_pj/GRP_la/JOB_i23/DIV_la7017049 DATE: September 18, 2007

Cell and Protein Compatibility of Parylene-C Surfaces

Tracy Y. Chang,[†,#] Vikramaditya G. Yadav,[‡,¶,#] Sarah De Leo,[§] Agustin Mohedas,[⊥] Bimal Rajalingam,[£] Chia-Ling Chen,[||] Selvapraba Selvarasah,[||] Mehmet R. Dokmeci,[||] and Ali Khademhosseini*,[£,¶]

Department of Biology, Massachusetts Institute of Technology, Cambridge, Massachusetts 02139, Department of Chemical Engineering, University of Waterloo, Waterloo, Canada N2L 3G1, Department of Biological Engineering, Louisiana State University, Baton Rouge, Louisiana 70808, Department of Biomedical Engineering, Texas A&M University, College Station, Texas 77843, Center for Biomedical Engineering, Department of Medicine, Brigham and Women's Hospital, Harvard Medical School, Boston, Massachusetts 02139, Department of Electrical and Computer Engineering, Northeastern University, Boston, Massachusetts 02115, and Harvard−MIT Division of Health Sciences and Technology, Massachusetts Institute of Technology, Cambridge, Massachusetts 02139

Received June 11, 2007. In Final Form: August 9, 2007

Parylene-C, which is traditionally used to coat implantable devices, has emerged as a promising material to generate miniaturized devices due to its unique mechanical properties and inertness. In this paper we compared the surface properties and cell and protein compatibility of parylene-C relative to other commonly used BioMEMS materials. We evaluated the surface hydrophobicity and roughness of parylene-C and compared these results to those of tissue culture-treated polystyrene, poly(dimethylsiloxane) (PDMS), and glass. We also treated parylene-C and PDMS with air plasma, and coated the surfaces with fibronectin to demonstrate that biochemical treatments modify the surface properties of parylene-C. Although plasma treatment caused both parylene-C and PDMS to become hydrophilic, only parylene-C substrates retained their hydrophilic properties over time. Furthermore, parylene-C substrates display a higher degree of nanoscale surface roughness (>20 nm) than the other substrates. We also examined the level of BSA and IgG protein adsorption on various surfaces and found that surface plasma treatment decreased the degree of protein adsorption on both PDMS and parylene-C substrates. After testing the degree of cell adhesion and spreading of two mammalian cell types, NIH-3T3 fibroblasts and AML-12 hepatocytes, we found that the adhesion of both cell types to surface-treated parylene-C variants were comparable to standard tissue culture substrates, such as polystyrene. Overall, these results indicate that parylene-C, along with its surface-treated variants, could potentially be a useful material for fabricating cell-based microdevices.

1. Introduction

Polymeric biomaterials are widely used in therapeutics[1,2] and diagnostics[3,4] as micro- and nanobiosensors for cell-based assays, drug delivery, and tissue-engineering applications.[5] Polymeric microdevices are capable for analyzing cells and proteins,[6−8] generating tissue-engineering scaffolds,[9−11] and miniaturizing bioassays for high-throughput experimentation.[12] With the recent emergence of soft lithography, elastomers, such as poly(dimethylsiloxane) (PDMS), have become enabling materials for the widespread fabrication and the use of microfabricated systems. PDMS offers numerous advantages over traditional biomaterials. It is relatively inexpensive, inert, nontoxic, and can be easily molded to form microstructures.[13] Despite these desirable characteristics, PDMS has a number of shortcomings. For example, although PDMS has been shown to be compatible for short-term culturing of cells,[14] little is known of its long-term stability in tissue-engineering applications and in vivo diagnostics. Therefore, it may be important to explore alternative biomaterials that can be used to fabricate biomedical microdevices. Poly-

* Corresponding author. E-mail: alik@mit.edu.
† Department of Biology, Massachusetts Institute of Technology.
‡ University of Waterloo.
§ Louisiana State University.
⊥ Texas A&M University.
£ Harvard Medical School.
|| Northeastern University.
¶ Harvard−MIT Division of Health Sciences and Technology, Massachusetts Institute of Technology.
# Denotes equal contributions.

(1) Langer, R. Drug delivery. Drugs on target. *Science* **2001**, *293* (5527), 58−59.
(2) Langer, R.; Vacanti, J. P. Tissue engineering. *Science* **1993**, *260* (5110), 920−926.
(3) Bashir, R. BioMEMS: state-of-the-art in detection, opportunities and prospects. *Adv. Drug Delivery Rev.* **2004**, *56* (11), 1565−1586.
(4) Byrne, M. E.; Park, K.; Peppas, N. A. Molecular imprinting within hydrogels. *Adv. Drug Delivery Rev.* **2002**, *54* (1), 149−161.
(5) Khademhosseini, A.; Langer, R.; Borenstein, J.; Vacanti, J. P. Microscale technologies for tissue engineering and biology. *Proc. Natl. Acad. Sci. U.S.A.* **2006**, *103* (8), 2480−2487.
(6) Folch, A.; Ayon, A.; Hurtado, O.; Schmidt, M. A.; Toner, M. Molding of deep polydimethylsiloxane microstructures for microfluidics and biological applications. *J. Biomech. Eng.* **1999**, *121* (1), 28−34.
(7) Khademhosseini, A.; Suh, K. Y.; Jon, S.; Eng, G.; Yeh, J.; Chen, G. J.; Langer, R. A soft lithographic approach to fabricate patterned microfluidic channels. *Anal. Chem.* **2004**, *76* (13), 3675−3681.
(8) Sia, S. K.; Whitesides, G. M. Microfluidic devices fabricated in poly(dimethylsiloxane) for biological studies. *Electrophoresis* **2003**, *24* (21), 3563−3576.
(9) Bianchi, F.; Vassalle, C.; Simonetti, M.; Vozzi, G.; Domenici, C.; Ahluwalia, A. Endothelial cell function on 2D and 3D micro-fabricated polymer scaffolds: applications in cardiovascular tissue engineering. *J. Biomater. Sci., Polym. Ed.* **2006**, *17* (1−2), 37−51.
(10) Fidkowski, C.; Kaazempur-Mofrad, M. R.; Borenstein, J.; Vacanti, J. P.; Langer, R.; Wang, Y. Endothelialized microvasculature based on a biodegradable elastomer. *Tissue Eng.* **2005**, *11* (1−2), 302−309.
(11) Kaihara, S.; Borenstein, J.; Koka, R.; Lalan, S.; Ochoa, E. R.; Ravens, M.; Pien, H.; Cunningham, B.; Vacanti, J. P. Silicon micromachining to tissue engineer branched vascular channels for liver fabrication. *Tissue Eng.* **2000**, *6* (2), 105−117.
(12) Thorsen, T.; Maerkl, S. J.; Quake, S. R. Microfluidic large-scale integration. *Science* **2002**, *298* (5593), 580−584.
(13) Whitesides, G. M.; Ostuni, E.; Takayama, S.; Jiang, X.; Ingber, D. E. Soft lithography in biology and biochemistry. *Annu. Rev. Biomed. Eng.* **2001**, *3*, 335−373.
(14) Lee, J. N.; Jiang, X.; Ryan, D.; Whitesides, G. M. Compatibility of mammalian cells on surfaces of poly(dimethylsiloxane). *Langmuir* **2004**, *20* (26), 11684−11691.

10.1021/la7017049 CCC: $37.00 © xxxx American Chemical Society
Published on Web 00/00/0000 PAGE EST: 7.7

(chloro-*p*-xylylene), also referred to as parylene-C, is one such potential candidate for fabricating biomedical devices.

Parylene-C is a thermoplastic, crystalline, and transparent polymer that is extensively used as a coating for insulating implantable biomedical devices.[15] In addition, parylene-C is chemically inert and nonbiodegradable. Parylene-C is synthesized from a low-molecular weight (MW) dimer, dichloro-di(*p*-xylylene), using a process that involves the decomposition of *p*-xylylene to yield chloro-*p*-xylylene, followed by the polymerization of chloro-*p*-xylylene to parylene-C.[16] Parylene-C can be vapor-deposited onto substrates to generate uniform, pinhole-free membranes that can be subsequently dry-etched using oxygen plasma to yield microscale features and patterns that are ideal for culturing cells.[17] The all-carbon structural backbone, high-MW, and nonpolar entities make parylene-C highly resistant to most chemicals, as well as to fungal and bacterial growth. In addition to having conducive biochemical properties, parylene-C has a Young's modulus of ~4 GPa[18] (compared to 0.75 MPa for PDMS[14])—making it mechanically robust and highly suitable for fabricating stable and reusable microfluidic devices or stencils.[17−22] Recent studies have shown parylene-C to be more hemocompatible and less thrombogenic than silicon.[23] Parylene-C has also demonstrated high stability in vivo for a variety of applications, such as cardiovascular implants.[24,25] Furthermore, parylene-C is a potentially useful material for in vitro cell culture studies. For example, we have developed the use of parylene-C stencils for patterning cells and proteins and for generation of cocultures with control over the degree of homotypic and heterotypic cell−cell interactions.[26,27] Another recent study provides the methodology for making nanoscale sculptured thin film (STF) out of parylene-C.[28] Due to the high surface area to volume ratio of the STF, the parylene-C STF supports high level of cell adhesion.[28] However, despite the apparent biocompatibility of parylene-C, there has been no direct comparison of parylene-C to PDMS and other materials commonly used in BioMEMS.

In this study, we compared the biocompatibility of parylene-C membranes with PDMS, glass, and optically clear virgin polystyrene by analyzing protein adsorption, cell adhesion, and cell morphology characteristics on each of these surfaces. In addition, we treated parylene-C and PDMS with air plasma and coated the surfaces of these substrates with fibronectin to study the effects of surface treatments on protein adsorption, cell adhesion, and spreading. Protein adsorption was studied using bovine serum albumin (BSA) and immunoglobulin G (IgG), and cell adhesion and spreading were studied using NIH-3T3 fibroblast and AML-12 hepatocyte cell lines.

2. Methods and Materials

2.1. Fabrication of Parylene-C and PDMS. Three inch silicon wafers were first cleaned for ~10 min using a 1:1 piranha solution (equal volume mixture of H_2SO_4 and H_2O_2), sufficiently rinsed with deionized water, nitrogen-dried, and then coated with hexamethyldisilazane (HMDS). Following pretreatment, the silicon wafers were deposited with dichloro-di(*p*-xylylene) by utilizing a Labcoater 2 PDS 2010 chemical deposition system (Specialty Coating Systems, Indianapolis). Inside the deposition system, dichloro-di(*p*-xylylene) is first vaporized at 150 °C and 1 torr and then pyrolyzed at 690 °C and 0.5 torr to form chloro-*p*-xylylene—the monomer of parylene-C. A reduction in the chamber temperature causes chloro-*p*-xylylene to condense onto the wafer surfaces to form parylene-C membranes. Initial loading of dichloro-di(*p*-xylylene) onto the silicon wafers determines the thickness of the parylene-C membrane at a rate of 0.5 μm/g. With the use of the aforementioned protocol, 10 μm thick parylene-C membranes were fabricated on silicon substrates.

The PDMS substrates were fabricated by directly curing a Sylgard 184 (Essex Chemical) elastomer in the wells of a Costar 24-well TC-treated cell culture microplate for nearly 2 h at 70 °C, using a 10:1 weight ratio of elastomer to curing agent.

2.2. Preparation of Surfaces. A total of eight types of surfaces were used in this study. Costar 24-well TC-treated cell culture microplates were utilized as optically clear virgin polystyrene substrates. Parylene-C experimental samples were prepared by carefully cutting the 10 μm thick parylene-C membranes (section 2.1) to form square-shaped pieces of ~5 mm × 5 mm. Each cut-out piece of parylene-C was placed and sealed reversibly onto a PDMS-coated well in the microplate. Platinum glass coverslips, 18 mm × 18 mm in size, were used as the glass samples. Plasma-treated PDMS and parylene-C were obtained by treating the two polymers with air plasma in a Harrick PDC-001 plasma treatment chamber for 2 min. Protein coating to parylene-C and PDMS surfaces was performed by simply incubating a 5 μg/mL fibronectin solution on the surfaces for 1 h.

Each substrate was sterilized prior to the experiments. The sterilization of plain and plasma-treated surfaces consisted of UV irradiation for 30 s, followed by successive washes with 70% ethanol and sterile PBS, respectively. The sterilization of fibronectin-coated surfaces consists of a 30 min of incubation of a sterile solution of fibronectin (5 μg/mL) on sterilized samples of plain PDMS and parylene-C.

2.3. Surface Property Characterization. *2.3.1. Contact Angle Measurements.* Contact angles were measured on static drops of water on different substrates by using a contact angle measurement system (Phoenix 300 plus, SEO) to provide information about hydrophobicity of the surfaces (See Table 1). The substrates were measured as-received or as-deposited (plain), and additional measurements were performed with a subset of these substrates (PDMS and parylene-C) that were treated with oxygen plasma and were coated with fibronectin. The contact angle measurements were performed by dispensing deionized water drops (5−10 μL) on each substrate with a micropipette (Ted Pella Inc.). Each data point represents an average of >10 independent measurements.

(15) Loeb, G. E.; Walker, A. E.; Uematsu, S.; Konigsmark, B. W. Histological reaction to various conductive and dielectric films chronically implanted in the subdural space. *J. Biomed. Mater. Res.* **1977**, *11* (2), 195−210.

(16) Hahn, A. W.; Yasuda, H. K.; James, W. J.; Nichols, M. F.; Sadhir, R. K.; Sharma, A. K.; Pringle, O. A.; York, D. H.; Charlson, E. J. Glow discharge polymers as coatings for implanted devices. *Biomed. Sci. Instrum.* **1981**, *17*, 109−113.

(17) Tooker, A.; Meng, E.; Erickson, J.; Tai, Y. C.; Pine, J. Biocompatible parylene neurocages. Developing a robust method for live neural network studies. *IEEE Eng. Med. Biol. Mag.* **2005**, *24* (6), 30−33.

(18) Chen, P. J.; Shih, C. Y.; Tai, Y. C. Design, fabrication and characterization of monolithic embedded parylene microchannels in silicon substrate. *Lab Chip* **2006**, *6* (6), 803−810.

(19) Licklider, L.; Wang, X. Q.; Desai, A.; Tai, Y. C.; Lee, T. D. A micromachined chip-based electrospray source for mass spectrometry. *Anal. Chem.* **2000**, *72* (2), 367−375.

(20) Meng, E.; Wu, S.; Tai, Y. C. Silicon couplers for microfluidic applications. *Fresenius' J. Anal. Chem.* **2001**, *371* (2), 270−275.

(21) Xie, J.; Miao, Y.; Shih, J.; Tai, Y. C.; Lee, T. D. Microfluidic platform for liquid chromatography-tandem mass spectrometry analyses of complex peptide mixtures. *Anal. Chem.* **2005**, *77* (21), 6947−6953.

(22) Xie, J.; Shih, J.; Lin, Q.; Yang, B.; Tai, Y. C. Surface micromachined electrostatically actuated micro peristaltic pump. *Lab Chip* **2004**, *4* (5), 495−501.

(23) Weisenberg, B. A.; Mooradian, D. L. Hemocompatibility of materials used in microelectromechanical systems: platelet adhesion and morphology in vitro. *J. Biomed. Mater. Res.* **2002**, *60* (2), 283−291.

(24) Schmidt, E. M.; McIntosh, J. S.; Bak, M. J. Long-term implants of parylene-C coated microelectrodes. *Med. Biol. Eng. Comput.* **1988**, *26* (1), 96−101.

(25) Eskin, S. G.; Armeniades, C. D.; Lie, J. T.; Trevino, L.; Kennedy, J. H. Growth of cultured calf aortic smooth muscle cells on cardiovascular prosthetic materials. *J. Biomed. Mater. Res.* **1976**, *10* (1), 113−122.

(26) Wright, D.; Rajalingam, B.; Karp, J.; Selvarasah, S.; Ling, Y.; Yeh, J.; Langer, R.; Dokmeci, M. R.; Khademhosseini, A. Reusable, reversibly sealable parylene membranes for cell and protein patterning. *J. Biomed. Mater. Res.* [Online early access]. DOI: 10.1002/jbm.a.31281.

(27) Wright, D.; Rajalingam, B.; Selvarasah, S.; Dokmeci, M. R.; Khademhosseini, A. Generation of static and dynamic patterned co-cultures using microfabricated parylene-C stencils. *Lab Chip* [Online early access]. DOI: 10.1039/b706081e.

(28) Demirel, M. C.; So, E.; Ritty, T. M.; Naidu, S. H.; Lakhtakia, A. Fibroblast cell attachment and growth on nanoengineered sculptured thin films. *J. Biomed. Mater. Res., Part B* **2007**, *81* (1), 219−223.

BATCH: la11a18 USER: sst29 DIV: @xyv04/data1/CLS_pj/GRP_la/JOB_i23/DIV_la7017049 DATE: September 18, 2007

Table 1. Contact Angle Measurements

substrates	contact angle (deg)		
	untreated	plasma-treated	fibronectin-coated
glass	36.3 ± 2.6		
polystyrene	79.1 ± 5.9		
PDMS	105.9 ± 4.5	9.9 ± 1.1[a] 73.7 ± 3[b]	99.0 ± 6.7
parylene-C	97.2 ± 4.2	4.4 ± 2.4[c]	105.0 ± 10.4

[a] Measurements made immediately after PDMS was treated in oxygen plasma. [b] Measurements made after 40 min following treatment in oxygen plasma. [c] No significant change observed in measurements made immediately after and following 40 min after plasma treatment.

Table 2. Surface Roughness Measurements

substrate	roughness (nm)
glass	1.6 ± 0.6
polystyrene	1.2 ± 0.2
parylene-C	19.3 ± 6.3
plasma-treated parylene-C	19.3 ± 5.4
fibronectin-coated parylene-C	29.0 ± 11.5
PDMS	2.2 ± 0.6
plasma-treated PDMS	0.4 ± 0.1
fibronectin-coated PDMS	3.2 ± 0.6

2.3.2. Surface Roughness Measurements. Surface roughness values of four different substrates (glass, polystyrene, PDMS, and parylene-C) as received were measured with atomic force microscopy (AFM) (Q-Scope 250, Quesant Instrument Corporation) using noncontact mode with a cantilever tip (NCS 16, Quesant). Scan areas of 50 μm × 50 μm were randomly selected on the substrates. To obtain the surface roughness values from an as-deposited thin (10 μm) parylene membrane, we first peeled the parylene off the silicon wafer and then placed it on top of a robust substrate (1 mm thick PDMS slab). Afterward, we performed the AFM measurements. To obtain the surface roughness of the surface-treated parylene-C, we applied surface treatments (O_2 plasma treatment or fibronectin coating) on the parylene surface mounted on a PDMS slab and performed AFM surface roughness measurements. Three independent measurements from 5 μm × 5 μm squares of each surface were performed and averaged. Roughness values (mean) acquired from various samples corresponding to the variations in surface heights are summarized in Table 2.

2.4. Protein Adsorption Measurements. Protein adsorption was characterized by incubating 50 μg/mL of fluorescein isothiocyanate (FITC)-conjugated BSA (Sigma-Aldrich) and 100 μg/mL of FITC-conjugated IgG (Sigma-Aldrich) on each substrate for 1 h. The substrates were encased in aluminum foil to prevent photodegradation of the FITC. Following incubation, the substrates were rinsed with deionized water and imaged using a fluorescent microscope (Nikon TE 2000) with a constant exposure time of 500 ms. Emitted fluorescence was then measured using ImageJ pixel brightness analysis tool (National Institutes of Health, U.S.A.). The average pixel brightness of each image is an indirect measurement of the protein adsorption onto the substrates. Control substrates were also used to eliminate the effect of autofluorescence from the substrates.

2.5. Cell Culture. NIH-3T3 fibroblasts were cultured in Dulbecco's modification of Eagle medium (DMEM) (Invitrogen) supplemented with 10% fetal bovine serum (Atlanta Biologicals) and 1% penicillin−streptomycin (MediaTech). AML-12 hepatocytes were preserved in 44.5% DMEM and 44.5% Ham's F12 media (Invitrogen) supplemented with 10% FBS and 1% penicillin−streptomycin (Sigma-Aldrich). The cells were maintained under humid conditions, at 37 °C, and in a 5% CO_2 atmosphere.

2.6. Preparation of Samples for Cell Adhesion. The NIH-3T3 fibroblasts and the AML-12 hepatocytes were trypsinized and resuspended in their respective media to form a 5 × 10^4 cells/mL stock solution. A volume of 2 mL of this stock solution was then incubated on each of the substrates for 6 h. Each well of the Costar 24-well microplate has a base area of 283.5 mm^2. This corresponds to a loading density of ∼353 cells/mm^2. Next, the substrates were rinsed twice with 1× phosphate-buffered saline (Invitrogen), and cells adhering to the substrates were then fixed using 4% paraformaldehyde (Sigma-Aldrich) and permeabilized with 0.2% Triton X-100 (Sigma) for 10 and 5 min, respectively.

2.7. Visualization and Imaging of Adhered Cells. To count the number of adhered cells on each surface, images of fluorescently labeled nuclei were collected using a fluorescent microscope (Nikon Eclipse TE 2000). Three pictures per well and three wells per substrate were analyzed and counted using ImageJ software.

2.8. Visualization and Imaging of Cells for Estimating Shape Factors. To analyze cell spreading on various surfaces, data was collected from at least 70 adhered cells per sample. To effectively analyze cell shape, the dimensionless shape factor, *S*, was used to compare the spreading of cells. It is computed as

$$S = 4\pi A/P^2$$

where *A* is the area occupied by the cell and *P* is the perimeter of the cell. A shape factor of 1 corresponds to a perfect circle, whereas a shape factor of 0 represents a line. Cell shape factors were computed utilizing the calibration and measurement features of the SPOT Imaging Software.

3. Results and Discussion

We evaluated the surface properties of parylene-C stencils in comparison with other commonly used biomedical materials, such as PDMS, glass, and polystyrene. In addition, we analyzed the effect of two common surface treatments, oxygen plasma and protein coating on these substrates. The surfaces were characterized for their hydrophobicity and roughness as well as for protein adsorption, cell adhesion, and cell morphology. Particular attention was paid to the differences between parylene-C and PDMS, due to their emerging applications in biomedical microfabrication.

3.1. Surface Analysis. Surface hydrophobicity and surface roughness are important factors in cell adhesion and the resulting cellular morphology.[14,29−31] In addition, hydrophobicity has also been shown to affect protein adsorption.[32−35] Therefore, it is important to evaluate these properties in parylene-C membranes to understand the interaction of mammalian cells with these substrates. To assess the hydrophobicity of the surfaces, we measured contact angles of as-deposited and treated parylene-C surfaces and compared the values to control surfaces (Table 1). The substrates varied greatly in their water contact angles, from ∼36° for glass to ∼111° for PDMS. As-deposited parylene-C and plain PDMS were both hydrophobic as they exhibited contact angles of ∼100°, which is consistent with our previous study.[36] Furthermore, fibronectin-coated parylene-C and PDMS were also hydrophobic (contact angles of ∼100°). This hydrophobic

(29) MacDonald, D. E.; Rapuano, B. E.; Deo, N.; Stranick, M.; Somasundaran, P.; Boskey, A. L. Thermal and chemical modification of titanium−aluminum−vanadium implant materials: effects on surface properties, glycoprotein adsorption, and MG63 cell attachment. *Biomaterials* **2004**, *25* (16), 3135−3146.

(30) Miller, D. C.; Thapa, A.; Haberstroh, K. M.; Webster, T. J. Endothelial and vascular smooth muscle cell function on poly(lactic-*co*-glycolic acid) with nano-structured surface features. *Biomaterials* **2004**, *25* (1), 53−61.

(31) Lee, J. H.; Lee, H. B. A wettability gradient as a tool to study protein adsorption and cell adhesion on polymer surfaces. *J. Biomater. Sci., Polym. Ed.* **1993**, *4* (5), 467−481.

(32) Toworfe, G. K.; Composto, R. J.; Adams, C. S.; Shapiro, I. M.; Ducheyne, P. Fibronectin adsorption on surface-activated poly(dimethylsiloxane) and its effect on cellular function. *J. Biomed. Mater. Res., Part A* **2004**, *71* (3), 449−461.

(33) Harnett, E. M.; Alderman, J.; Wood, T. The surface energy of various biomaterials coated with adhesion molecules used in cell culture. *Colloids Surf., B* **2007**, *55* (1), 90−97.

(34) Warkentin, P.; Walivaara, B.; Lundstrom, I.; Tengvall, P. Differential surface binding of albumin, immunoglobulin G and fibrinogen. *Biomaterials* **1994**, *15* (10), 786−795.

(35) Absolom, D. R.; Zingg, W.; Neumann, A. W. Protein adsorption to polymer particles: role of surface properties. *J. Biomed. Mater. Res.* **1987**, *21* (2), 161−171.

BATCH: la11a18 USER: sst29 DIV: @xyv04/data1/CLS_pj/GRP_la/JOB_i23/DIV_la7017049 DATE: September 18, 2007

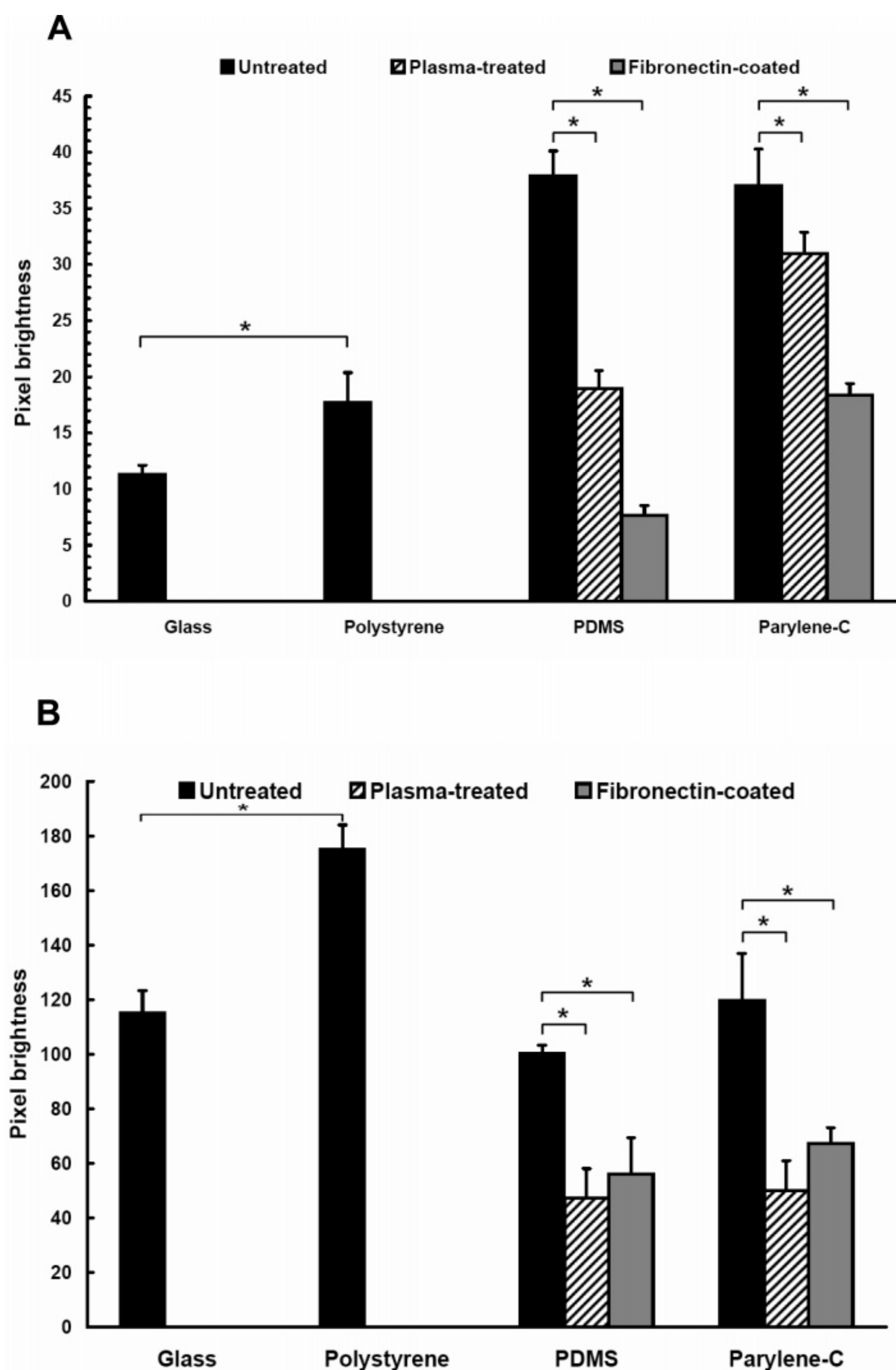

Figure 1. Adsorption of FITC−BSA (A) and FITC−IgG (B) onto each of the substrates. (A) Adsorption of FITC−BSA onto parylene-C and PDMS exceeds that on glass and polystyrene. Surface modifications of parylene-C and PDMS show a negative effect on FITC−BSA adsorption. (B) FITC−IgG adsorbs onto glass, parylene-C, and PDMS in a comparable manner. Adsorption onto polystyrene is the highest. Surface modification of parylene-C and PDMS reduces their affinity for FITC−IgG. In general, plasma treatment and fibronectin coating the two polymers reduces their ability to adsorb proteins. The ∗ indicates $p < 0.05$.

240 property of fibronectin-coated PDMS is confirmed by results
241 obtained by other groups.[32] Even though there has not been
242 investigation in the past on fibronectin-coated parylene-C, it is
243 logical to expect it to be hydrophobic. Because fibronectin
244 coatings have no electron donor components and have low surface
245 energy,[33] materials coated with fibronectin would not form
246 hydrogen bonds with water molecules, so they would become
247 hydrophobic. Furthermore, air plasma treatment reduced the
248 contact angle of both parylene-C and PDMS substrates to less
249 than 10°. This finding agrees well with the previous findings that
250 the formation of hydroxyl groups from the O_2 plasma treatment
251 process significantly increases the hydrophilicity of surfaces.[8]

252 One of the main drawbacks of using PDMS for fluidic devices
253 is that the plasma-induced hydrophilicity of the PDMS surfaces
254 is short term.[7] In many applications involving fluidics and cells,
255 the ability to generate substrates that remain hydrophilic may be
256 beneficial. To compare the stability of plasma-treated surfaces,
257 we measured the contact angles of plasma-treated parylene-C
258 and PDMS surfaces immediately and 40 min after plasma
259 treatment. It was observed that although the plasma treatment

(36) Selvarasah, S.; Chao, S. H.; Chen, C. L.; Mao, D.; Hopwood, J.; Ryley, S.; Khademhosseini, A.; Busnaina, A.; Dokmeci, M. R. A high aspect ratio, flexible, transparent and low-cost parylene-C shadow mask technology for micro patterning applications. Presented at the 14th International Conference on Solid-State Sensors, Actuators and Microsystems, Lyon, France, 2007; 533−536.

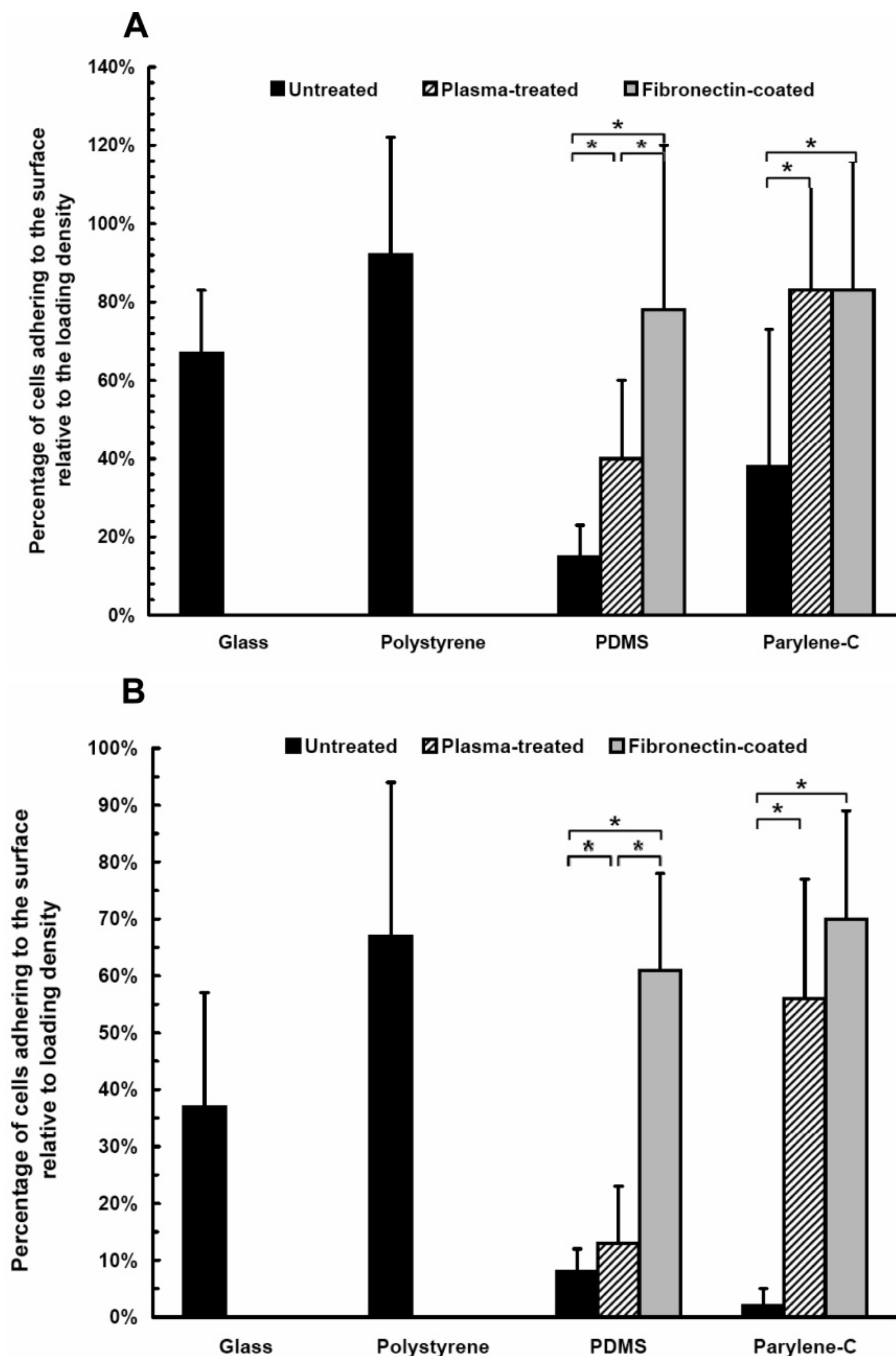

Figure 2. Adhesion of (A) NIH-3T3 fibroblasts and (B) AML-12 hepatocytes on the various substrates. (A) The cells do not adhere to as-deposited parylene-C and plain PDMS. Furthermore, plasma treatment and fibronectin coating of the two polymers increase their adhesiveness to NIH-3T3 cells. (B) Similar trends are exhibited by AML-12 adhesion to the various substrates. The ∗ indicates $p < 0.05$.

initially decreased the contact angle values, the hydrophilicity of a PDMS substrate deteriorated rapidly (Table 1). This is due to the viscoelastic properties of PDMS, in which the surface molecules "turn over" with time exposing non-plasma-treated molecules of the PDMS on its surface. On the other hand, the contact angle for plasma-treated parylene-C did not change significantly after 40 min. The fact that the plasma-treated parylene surface stays hydrophilic for longer periods could be advantageous

BATCH: la11a18 USER: sst29 DIV: @xyv04/data1/CLS_pj/GRP_la/JOB_i23/DIV_la7017049 DATE: September 18, 2007

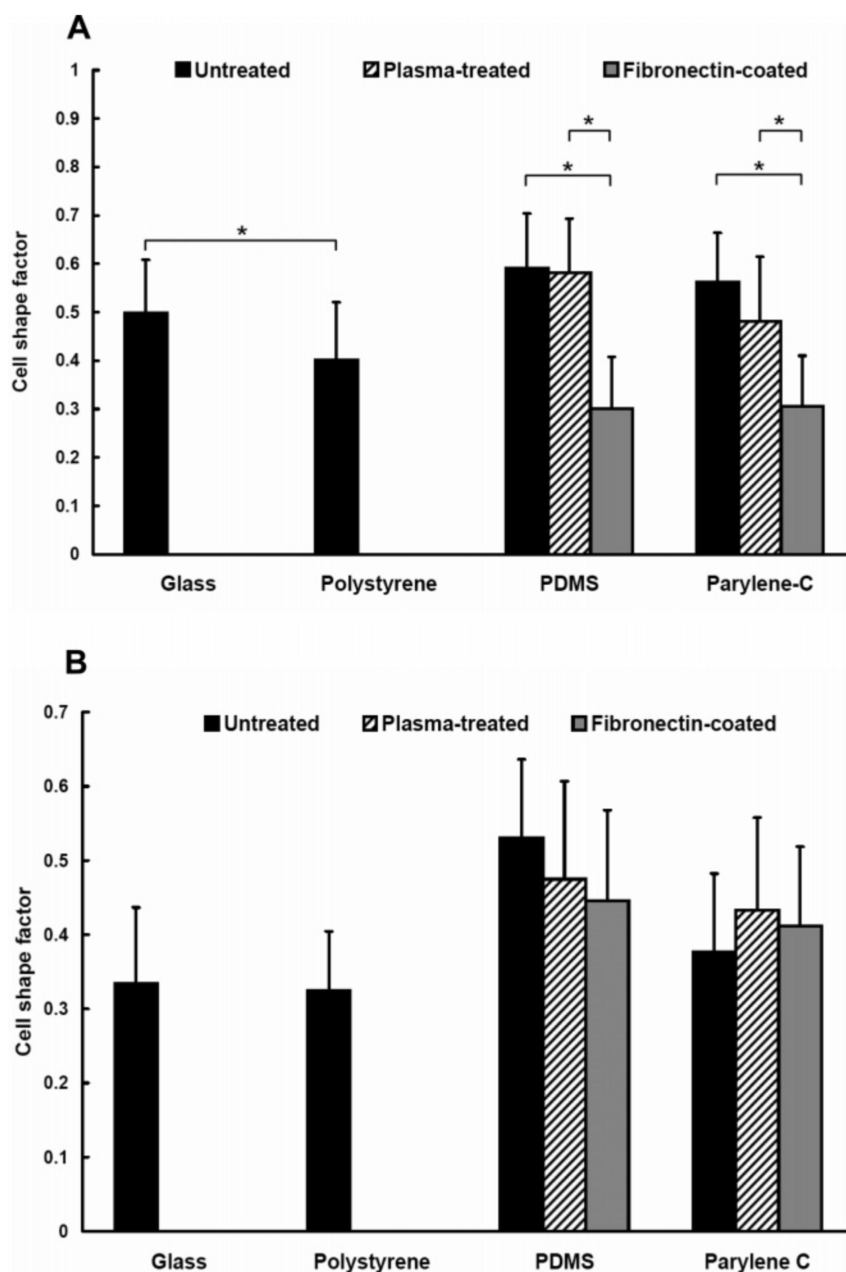

Figure 3. Dimensionless cell shape factor measurements for (A) NIH-3T3 fibroblasts and (B) AML-12 hepatocytes cultured on various substrates. (A) NIH-3T3 cells exhibit greater spreading on fibronectin-coated parylene-C and PDMS, as compared to the other substrates. (B) Due to nonaxial spreading, shape factor was not an adequate measurement of AML-12 proliferation on the surfaces, and ANOVA was not conducted on this data. The $*$ indicates $p < 0.05$.

268 for various biological applications. We next examined the surface 269 roughness of the parylene-C and PDMS substrates by using AFM. 270 As shown in Table 2, as-deposited and treated parylene-C 271 substrates were significantly rougher compared to other substrates, 272 including glass, PDMS, and polystyrene. Fibronectin-treated 273 parylene-C surfaces had the highest roughness values of ~30 274 nm. The higher surface roughness values of parylene-C may be 275 due to the irregularities in the deposition process, which were 276 further increased with fibronectin molecules adsorbed onto the 277 surface. On the other hand, PDMS, glass, and polystyrene were 278 much smoother with surface roughness values of <3 nm. An 279 increase in surface roughness enhances the protein adsorption 280 level, since there is more available surface area for proteins to 281 attach.[29] When there are more proteins adsorbed onto the surface, 282 more integrin receptors on the cells will bind to the proteins and, 283 therefore, mediate the attachment of cells.[29]

3.2. Protein Adsorption. To generate substrates that are 284 favorable for cell adhesion, a routine procedure is to coat a layer 285 of adhesive proteins on the substrates. To measure protein 286 adsorption properties of parylene-C relative to other substrates, 287 we incubated each sample with fluorescently labeled BSA and 288 IgG. First observation we made was that significantly more BSA 289 and IgG adsorbed to polystyrene relative to glass. This finding 290 is consistent with other studies that BSA and IgG adsorb more 291 onto highly hydrophobic surfaces like polystyrene, compared to 292 relatively hydrophilic surfaces like glass.[14,29,31,33] Similarly, BSA 293 adsorption level on plain PDMS and as-deposited parylene-C 294 were 3 times higher relative to glass (Figure 1A). On the other 295 hand, IgG adsorption levels on plain PDMS and as-deposited 296 parylene-C were similar to adsorption on glass. We believe that 297 this discrepancy is caused by the intrinsic difference in the 298 structure of two proteins. 299

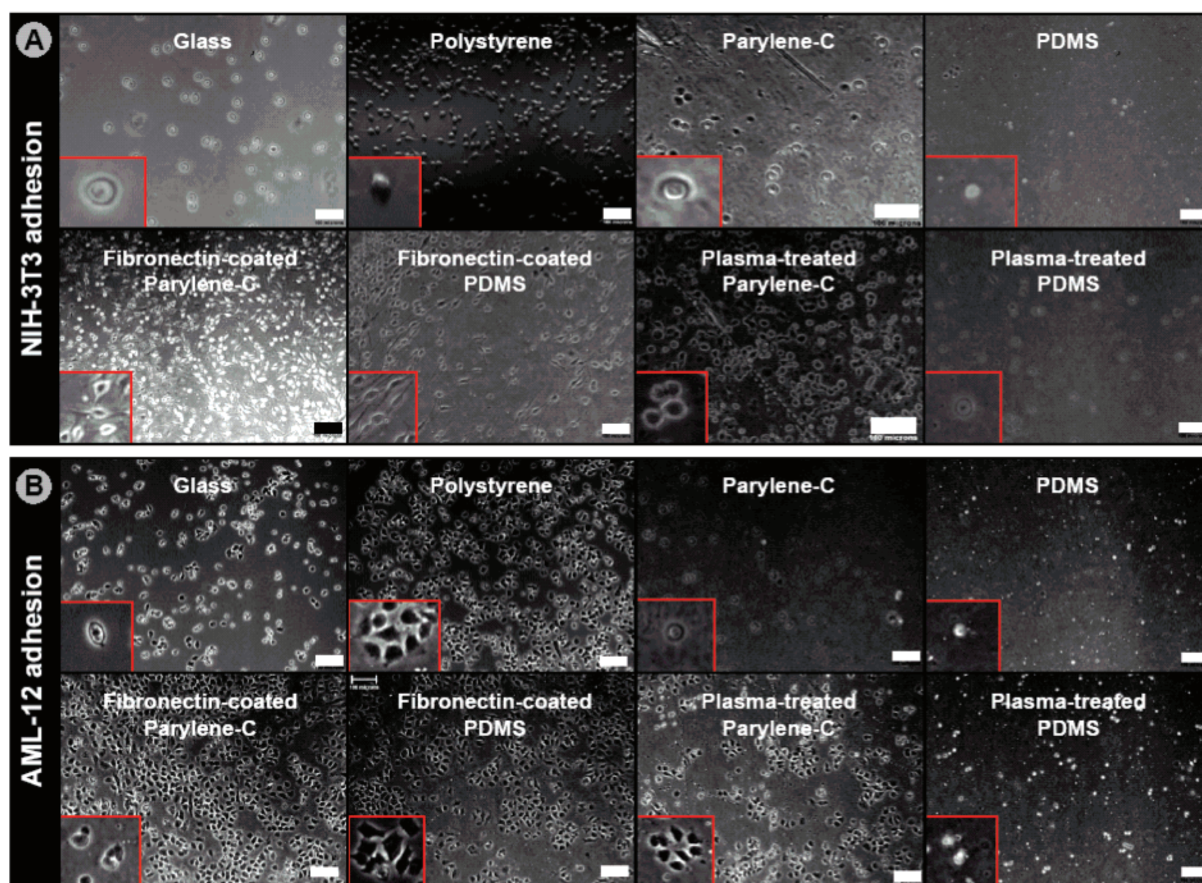

Figure 4. Micrographs of NIH-3T3 fibroblasts (A) and AML-12 hepatocytes (B) on various surfaces. The insets contain images which have been cropped and magnified for optimal viewing. Scale bar = 100 μm.

In addition, we analyzed the effects of plasma treatment and initial protein coating on IgG and BSA adsorption. Plasma treatment is routinely used to increase the surface hydrophilicity of materials, such as PDMS and polystyrene, and can be used to modify the surface of parylene-C substrates (Table 1). In our studies, plasma treatment of parylene-C and PDMS increased the hydrophilicity of the surfaces and reduced the adhesion of both BSA (Figure 1A) and IgG (Figure 1B). This is because of increased hydrogen bonding between the surface and water molecules, which displaces the weak electrostatic interaction and hydrophobic interactions between serum proteins and the surface.[33] In addition, fibronectin coatings, which improve cellular adhesion on biomaterials, could also be used to minimize the subsequent adsorption of BSA and IgG. This can be explained by the fact that the adsorption of the first layer of protein results in the creation of a thermodynamically stable interface of water molecules coupled with the hydrophilic regions of the adsorbed protein layer.[34] This phenomenon is commonly used in immunoassays, in which an adsorbed layer of protein is applied to minimize background adsorption of the antibody to the substrate.[34]

Thus, our results indicate that as-deposited parylene-C has high BSA and IgG adsorption, while surface treatments on parylene-C can be used to decrease levels of adsorption of these proteins. The ability to modify the level of protein adsorption on the parylene-C substrates is of potential value for various biomedical applications and microfabrication techniques.

3.3. Cell Adhesion and Spreading. To evaluate the cytocompatibility of parylene-C substrates relative to other materials, we analyzed the adhesion of and spreading of fibroblast (NIH-3T3) and hepatocyte (AML-12) cell lines. In these experiments, cells were seeded on various surfaces and incubated for 6 h, and the adherent cells were counted and measured. In Figure 2, parts A and B, varying levels of cell adhesion on the different substrates were displayed. Interestingly, both plain PDMS and as-deposited parylene-C substrates heavily repelled cell adhesion for both NIH-3T3 and AML-12 cells. On both surfaces, cells remained in round shape and could be easily washed away. These substrates were significantly less adhesive to cells than tissue culture polystyrene and glass controls.

To investigate how surface treatments influence cell adhesion, we examined the effects of plasma treatment and fibronectin coating on the parylene-C and PDMS substrates. It was found that both treatments resulted in an increase in the cell adhesiveness of the substrates. Previously, it has been demonstrated that plasma-treated PDMS surfaces display enhanced cell adhesion.[14,29,31] Also, fibronectin, which is an extracellular matrix component that mediates cell adhesion and spreading, has been used extensively to increase cell adhesion.[32] As expected, the adhesion levels of both NIH-3T3 and AML-12 cells on surface-modified substrates (via plasma treatment and fibronectin coatings) were significantly enhanced as shown in Figure 2, parts A and B. Interestingly, there was a difference in cell adhesion levels between plasma-treated and fibronectin-coated PDMS, whereas no significant change was observed for parylene-C substrates. This phenomenon can be caused by the temporary effect of plasma treatment on PDMS compared with the longer lasting effect of plasma treatment on parylene-C (Table 1). Therefore, it may be that as the plasma-induced hydrophilicity of the PDMS substrates is decreased, plasma-treated PDMS was less favorable to cell adhesion. In comparison, plasma-treated parylene-C remained hydrophilic and suitable for cell adhesion. These results demonstrate that even though as-deposited parylene-C substrates

362 are relatively rough (>20 nm) and hydrophobic, and cells do not
363 adhere onto these surfaces. Furthermore, it is possible to increase
364 the surface-adhesive properties simply by surface treatment
365 approaches such as plasma treatment and fibronectin coating.
366 In addition to analyzing the number of cells adhering onto the
367 various surfaces, we also examined the degree of cell spreading.
368 The level of spreading is important because it influences various
369 parameters, such as cellular proliferation and differentiation.[32]
370 To determine the degree of cell spreading on different substrates,
371 we quantified cell morphology by calculating a dimensionless
372 shape factor with the results illustrated in Figure 3. The
373 dimensionless shape factor ranges from zero (line—for linearly
374 spread cell) to one (circle—for cells that have not elongated) and
375 can be used to validate the degree of cell adhesiveness on a
376 surface. It is then only appropriate to use this shape factor to
377 quantify cell spreading if the adhered cells display axial spreading.
378 Note that, whereas NIH-3T3 cells spread along a single axis,
379 AML-12 cells spread more uniformly with extended pseudopodia,
380 therefore exhibiting inherently higher shape factors. Phase
381 micrographs of both NIH-3T3 and AML-12 cells are displayed
382 in Figure 4. Randomly selected cells from each image were
383 chosen and traced using SPOT imaging software to emphasize
384 the differences in cell morphology among the various substrates.
385 The results indicate that NIH-3T3 cells spread well on
386 fibronectin-coated parylene-C and PDMS as well as tissue culture-
387 treated polystyrene (Figure 3A). As for plasma-treated parylene-C
388 and PDMS, a small fraction of NIH-3T3 cells on these substrates
389 exhibited adhered and spread morphologies, whereas the rest
390 maintained their circular phenotype. The majority of NIH-3T3
391 cells on plain substrates of parylene-C, PDMS, and glass remained
392 circular. On the other hand, since all AML-12 cells adhered in
393 a nonelongated manner, their cell shape factor values were higher
394 and similar in value (Figure 3B). As a result, cell shape factor
395 is not a conclusive measure of spreading of AML-12 cells.
396 The cell adhesion and morphology on as-deposited parylene-C
397 and plain PDMS substrates were not significantly different
398 (Figures 2 and 3), despite a clear difference in surface roughness
399 between the two materials (Table 2). Several studies have
400 concluded that increasing the surface roughness increases the
401 levels of cell adhesion and spreading.[25,29,32] However, after
402 comparing the level of cell adhesion and spreading between
403 as-deposited parylene-C and plain PDMS substrates, we believe
404 that the intrinsic differences between materials outweighed the
405 effect of surface roughness. Therefore, future biocompatibility
406 studies that utilize different polymeric substrates with varying
407 levels of surface roughness are required to fully clarify this matter.
408 Overall, we have found that plasma-treated and fibronectin-
409 coated parylene-C membranes were as compatible for cell culture
410 as commonly used substrates such as glass and polystyrene. The
411 ease with which as-deposited surfaces can be made cell adhesive
412 and the cell-resistant property of as-deposited parylene-C may
413 potentially be useful in biomedical applications. Similarly, these
414 substrates can be engineered to enhance or reduce protein
415 adsorption which is conducive to biological research. Long-term
416 studies on the biocompatibility and more comprehensive trials
417 with other proteins and cell types might be necessary to fully
418 understand the benefits and limitations of parylene-C.

4. Conclusions 419

420 Although parylene-C has been used as a biologically inert
421 coating on implantable devices for many years, there had not
422 been systematic studies of the biocompatibility of parylene-C
423 and its surface-treated variants. In this paper, we have compared
424 parylene-C to other commonly used cell culture substrates and
425 demonstrate that surface-treated parylene-C substrates exhibit
426 adhesion levels comparable to commercially available tissue
427 culture-treated polystyrene. On the other hand, as-deposited
428 parylene-C substrates, which are not cell adhesive, can be used
429 as restrictive coating to minimize cell adhesion. Overall,
430 parylene-C can easily be surface modified into a suitable substrate
431 for culturing mammalian cells. Given that parylene-C has already
432 been shown to be well suited for microfabrication, and that it can
433 be made into flexible and robust devices, the data presented here
434 would be useful for the implementations that tailor to the
435 biocompatibility of parylene-C. The new implementations of
436 parylene-C will likely lead to new technologies and devices for
437 biomedical applications.

438 **Acknowledgment.** The authors acknowledge funding from
439 the Institute for Soldier Nanotechnology, the Coulter Foundation,
440 the Center for Integration of Medicine and Innovative Technology
441 (CIMIT), National Institutes of Health (NIH), and the Draper
442 Laboratory. We thank Vahik Krikorian for technical support.

443 LA7017049